# Production of neutrons up to 18 MeV in high-intensity, short-pulse laser matter interactions

D. P. Higginson, J. M. McNaney, D. C. Swift, G. M. Petrov, J. Davis et al.

Citation: Phys. Plasmas **18**, 100703 (2011); doi: 10.1063/1.3654040
View online: http://dx.doi.org/10.1063/1.3654040
View Table of Contents: http://pop.aip.org/resource/1/PHPAEN/v18/i10
Published by the American Institute of Physics.

# Production of neutrons up to 18 MeV in high-intensity, short-pulse laser matter interactions

D. P. Higginson,[1,2] J. M. McNaney,[2] D. C. Swift,[2] G. M. Petrov,[3] J. Davis,[3] J. A. Frenje,[4] L. C. Jarrott,[1] R. Kodama,[5] K. L. Lancaster,[6] A. J. Mackinnon,[2] H. Nakamura,[5] P. K. Patel,[2] G. Tynan,[1] and F. N. Beg[1]
[1]*Mechanical and Aerospace Engineering, University of California-San Diego, La Jolla, California 92093, USA*
[2]*Lawrence Livermore National Laboratory, Livermore, California 94440, USA*
[3]*Naval Research Laboratory, Plasma Physics Division, Washington, DC 20375, USA*
[4]*Plasma Science and Fusion Center, Massachusetts Institute of Technology, Cambridge, Massachusetts 02139, USA*
[5]*Institute of Laser Engineering, Osaka University, 2-5 Yamada-oka, Suita, Osaka 454-0871, Japan*
[6]*STFC Rutherford Appleton Laboratory, Chilton, Oxon OX11OQX, United Kingdom*

(Received 29 June 2011; accepted 29 September 2011; published online 24 October 2011)

The generation of high-energy neutrons using laser-accelerated ions is demonstrated experimentally using the Titan laser with 360 J of laser energy in a 9 ps pulse. In this technique, a short-pulse, high-energy laser accelerates deuterons from a $CD_2$ foil. These are incident on a LiF foil and subsequently create high energy neutrons through the $^7$Li(d,xn) nuclear reaction ($Q = 15$ MeV). Radiochromic film and a Thomson parabola ion-spectrometer were used to diagnose the laser accelerated deuterons and protons. Conversion efficiency into protons was 0.5%, an order of magnitude greater than into deuterons. Maximum neutron energy was shown to be angularly dependent with up to 18 MeV neutrons observed in the forward direction using neutron time-of-flight spectrometry. Absolutely calibrated CR-39 detected spectrally integrated neutron fluence of up to $8 \times 10^8$ n sr$^{-1}$ in the forward direction. © *2011 American Institute of Physics*.
[doi:10.1063/1.3654040]

The generation of neutrons with energies in excess of 10 MeV is of great interest due to demanding applications, such as fusion power plant materials testing,[1] contraband detection,[2] and fissile material waste disposal,[3] among others.[4,5] These applications require a high flux of neutrons, which is possible with nuclear reactors, spallation sources, and particle accelerators. Unfortunately, these devices not only take up significant space but also extremely expensive to build and maintain [see Ref. 1 for details]. High-intensity, petawatt class lasers may provide an attractive alternate with relatively lower costs, which is timely due to the rapid advance of high repetition rate, high energy lasers.[6]

It has previously been demonstrated experimentally that high-intensity lasers can be used to produce neutrons by directly accelerating deuterons through thick deuterated targets[7] or using accelerated protons impinging on a secondary target.[4,5] However, due to low exothermic reaction energies, these studies were limited to neutron energies below 3 MeV. Perkins *et al.*[1] proposed a conceptual design of producing neutrons above 10 MeV using deuterium-tritium targets, though no experiments were carried out to implement this design. Recently, a new scheme was proposed by Davis and Petrov *et al.*[8] to generate neutrons in excess of 10 MeV by accelerating deuterons and interacting them with Lithium or other low Z materials. This technique has the advantage of producing higher and more directional neutron fluence, but experiments had not yet been carried out to validate these predictions.

In this letter, we present the first experimental results of the production of neutrons with energies up to 18 MeV using high-energy, short pulse lasers. Spectrally integrated fluence of up to $8 \times 10^8$ n sr$^{-1}$ was measured.

This experiment was performed at the Jupiter Laser Facility at the Lawrence Livermore National Laboratory (LLNL) using the Titan laser. Titan is an Nd:glass, $\lambda = 1.05$ $\mu$m, laser with a 15 $\mu$m diameter focal spot containing 50% of the laser energy. The laser energy was 360 J and the pulse length was 9 ps, giving a peak intensity of $2 \times 10^{19}$ W/cm$^2$. The inset of Figure 1 shows the target setup to create neutrons. The laser was incident on a 25 $\mu$m $CD_2$ foil at 16.5°, which accelerated ions from the rear surface of the foil through the target-normal sheath acceleration (TNSA) mechanism.[9] Since the TNSA mechanism is more effective for ions with large charge-to-mass ratios,[10] protons (from a contaminant layer on the target) are preferentially accelerated over other ion species. These ions were then incident on a 1.8 mm LiF slab placed 1 mm away from the foil, where they generated neutrons through nuclear reactions in the LiF. The target setup to diagnose the ion beam was similar with the exception of the LiF slab.

Radiochromic film (RCF) stacks were used to measure the absolute spectrum of the proton beam. RCF is an absolutely calibrated[11] film that is sensitive to ions. Alternating layers of RCF and Al were placed 9 cm from the target and resolved energies from 5.1 to 36 MeV. The lowest energy was set to avoid contamination by other ions. While some deuterons deposit energy in the RCF, they are much lower in number than the protons and can be neglected. The proton spectrum was fit with a Maxwellian energy spectrum

 

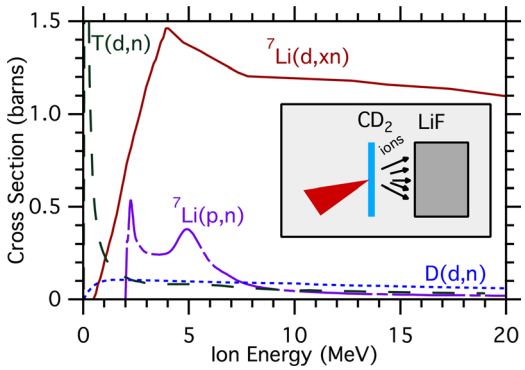


FIG. 1. (Color online) Cross sections of nuclear reactions that have potential for neutron generation using ions. Above 1 MeV the $^7$Li(d,xn) reaction is the highest by far. The inset shows the target setup used in this experiment, where ions accelerated from a $CD_2$ foil are incident on a LiF slab.

$dN/dE = (N/\sqrt{\pi ET})e^{-E/T}$ where the best fit was given with $N = 3.2 \times 10^{13}$, $T = 2.5$ MeV, with a cutoff energy of 16.6 MeV, which gives a conversion efficiency into protons above 5.1 MeV of 0.47%. The largest error in the RCF comes from batch to batch error which is 10%.[11]

RCF cannot discriminate between different ion species due to its sensitivity to all ions. Thus a Thomson Parabola ion-spectrometer (TPIS) was employed to measure deuteron and proton spectra passing through a small pinhole of approximately 90 $\mu$m diameter placed 60 cm from the target in the center of the ion beam. The TPIS uses parallel magnetic and electric fields to deflect ions, which are then incident on a Fujifilm TR imaging plate (IP). The resulting tracks follow a parabolic curve that is determined by the charge-to-mass ratio of the ions (see Carroll *et al.*[12] for the design of this diagnostic).

A 25 $\mu$m Al foil was placed in front of the IP to stop carbon ions below 24.5 MeV. This prevented overlapping of the $^{12}C^{6+}$ ion and deuteron tracks, as they have identical charge-to-mass ratios. The absence of other carbon ion species makes it unlikely that many $^{12}C^{6+}$ ions with energies above 24.5 MeV reached the IP. Traces from two targets are shown on the left side of Figure 2. The oscillations in the ion traces are due to electromagnetic interference generated by the laser pulse.

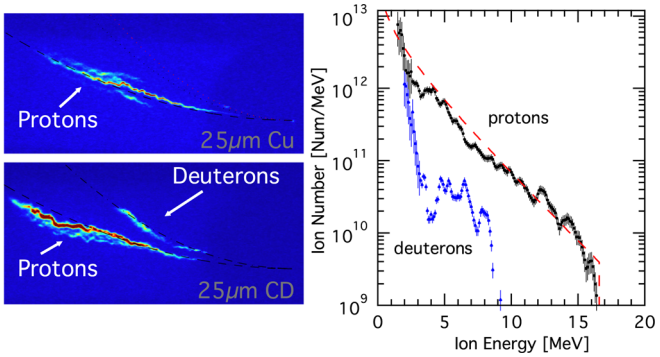


FIG. 2. (Color online) The left side shows false color traces from the TPIS of a Cu foil (top) and a $CD_2$ foil (bottom). The right side shows the proton spectrum as measured using RCF (dotted line), as well as spectra of protons (squares) and deuterons (triangles) taken from the TPIS, which have been normalized to the RCF data (all from Shot 18).

Two issues must be addressed to get quantitative data from the TPIS. First, the energy dependent response of the TR IPs must be inferred and second, the absolute number of deuterons must be determined. The energy dependent response was found by calculating the amount of energy an incident deuteron deposits in the active layer of the IP using the collisional Monte-Carlo code SRIM.[13] The technique matched well with experimentally determined calibrations[14] as long as the proton had enough energy to completely exit the active layer of the IP. This corresponds to 1.7 MeV for protons and 2.1 MeV for deuterons. Below this energy deviations of up to 50% were observed. Error bars were determined by combining the statistical error of the signal with the error from our energy deposition model. Differences in IP response that are independent of energy deposition have been ignored. To determine the absolute number of deuterons, the TPIS was cross correlated with the RCF stacks by comparing the proton signal on both detectors on the same shot. Note that this method does not account for differences in the spatial profile between the proton and deuteron beams. We obtained the conversion efficiency into deuterons above 3.1 MeV of 0.04%, by integrating the amount of energy in this spectrum. The 3.1 MeV limit is set by the energy a deuteron requires to pass through the Al filter and the IP active layer completely.

Both the conversion efficiency and maximum deuteron energy is lower than that of protons. This observation is consistent with modeling,[15] which suggests that, in deuterated targets with contaminant layers, the electric potential is screened from the interior of the target by the (outer) contaminant layer. Thus, the deuterons are not accelerated with the same force or for the same duration as the protons, leading to reduced number and energy.

Once accelerated, these ions are incident on a LiF slab. As the ions are stopped within the LiF, they undergo (p,n) and (d,n) nuclear reactions (see Figure 1) producing neutrons. The highest energy neutrons will be produced by elastic $^7$Li(d,xn) reactions. The $Q$-value for this reaction is 15 MeV, however there is a high probability to excite residual levels in the resultant $^8$Be nucleus, which will result in lower energy neutrons as compared to elastic reactions.[16]

To determine the neutron energy spectrum, neutron time-of-flight spectrometers (nTOF) were placed 4.54 m and 4.69 m away from the target at 17.5° and 157.5° from target normal, respectively. The nTOFs measure the travel time of neutrons from source to detector to deduce their kinetic energy. The neutron signal was measured with a quenched BC422Q scintillator coupled to a photomultiplier tube (Hamamatsu R2083). The scintillator is cylindrical with a diameter of 18 cm and thickness 2.5 cm. In the short pulse laser environment, hot electrons produce copious x-rays that cause scintillation events and can potentially saturate the detector. Shielding of 15.2 cm (front) and 25.4 cm (rear) of Pb was placed in front of the scintillators to avoid saturation. This shielding caused neutrons to scatter considerably. For this reason, extracting an accurate neutron spectrum is difficult and we focus only on determining the maximum neutron energy, as these neutrons arrive at the detectors first and, therefore, can be measured above the scattering. We estimate

the neutron detection limit to be on the order of $10^6$ n sr$^{-1}$. This is done by determining the signal level that is visible above the noise floor and then deducing the neutrons required to produce this signal by comparing the integrated nTOF spectrum with the CR-39 results.

Figure 3 shows the raw nTOF data from the front and the rear detectors. The initial peak that falls off quickly is caused by x-rays interacting with the scintillator and the peak around 80–100 ns is caused by the highest energy neutrons. In the inset of Figure 3, the upper axis has been converted to neutron energy using the relativistic energy equation. Figure 3 also includes a shot where no LiF converter foil was used. This shot indicates that a significant number of neutrons were produced through D(d,n) reactions in the $CD_2$ foil. Additionally, the many incident protons will also produce neutrons through the $^7$Li(p,n) reaction. However, neither of these reactions will produce high-energy neutrons due to the low $Q$-values of 3.3 MeV and −1.6 MeV of the D(d,n) and $^7$Li(p,n) reactions, respectively. Therefore these reactions make an insignificant contribution to the neutrons above 10 MeV. The maximum neutron energies are shown in Figure 4 and indicate maximum neutron energies of 18 MeV and 13 MeV in the forward and backward directions, respectively.

By determining the resultant angular distribution of neutron energy from elastic collisions, we find that our results fit well with an effective deuteron energy of 3 MeV, as shown in Figure 4. This may seem to contradict the 8 MeV maximum deuteron energy observed on the TPIS, however the neutron production probability is small compared to the stopping power in LiF. Thus, most deuterons will have slowed significantly before they produce neutrons. Additionally, the probability of an inelastic interaction is much greater than the probability of an elastic interaction for deuterons in Li.[16] Also, the deuteron spectrum is exponential so the majority of ions reside at lower energies. None of these effects prevent 8 MeV deuterons from generating neutrons from elastic interactions, but the number of neutrons may be decreased to a level that was below the nTOF detection limit.

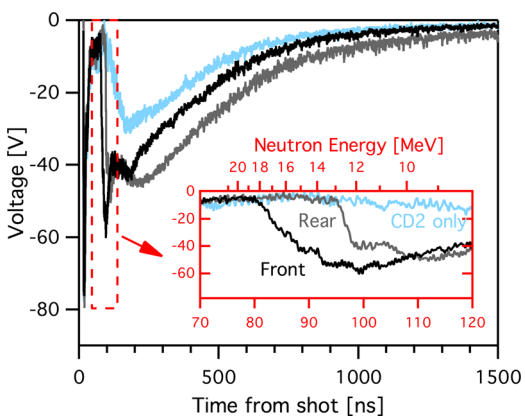


FIG. 3. (Color online) The main figure shows smoothed raw traces from the nTOF diagnostic on Shot 9. The darker and lighter lines are from the front (away from laser), 17.5°, and rear nTOFs, 157.5°, respectively. The lightest line shows a shot from the front nTOF taken by shooting only $CD_2$ without a LiF converter (Shot 18). The inset shows a magnified portion of the signal, where the upper axis has been converted to neutron energy.

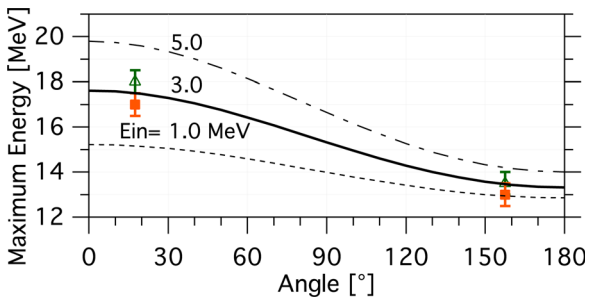


FIG. 4. (Color online) Maximum neutron energies. The green triangles (Shot 9) and orange squares (Shot 4) show data with the same nominal laser parameters (i.e., 360 J, 9 ps). The lines show the (maximum) neutron energy expected through elastic interactions with varied incident deuteron energies, Ein.

Three stacks of three layers of CR-39 detectors were placed 4.5 to 8 cm away from the target at 0°, 90°, and 135° relative to target normal to diagnose the absolute neutron number. CR-39 is a scratch resistant plastic that is insensitive to x-rays and electrons. CR-39 is damaged indirectly by neutrons through knock-on protons that leave damage tracks. After etching with NaOH these tracks can be seen under a microscope. To prevent proton contamination, 9.5 to 12.5 mm of Al was placed in front of the CR-39. The CR-39 was calibrated at LLNL with a $^{252}$Cf source. While this spectrum is not identical to the one produced in our experiment, the difference in average sensitivity was found to be negligible by comparing the expected experimental (calculated as in Ref. 8) and calibration spectra with respect to CR-39 sensitivity. The shielding setup for the calibration and the experiment were identical so that neutron scattering could be ignored. The neutron fluence, as observed by the CR-39, is shown in Figure 5. Error bars are determined from the uncertainty in the calibration and the deviation of layers within the CR-39 stack. As shown in the nTOF spectra, there was significant neutron generation through D(d,n) processes in the $CD_2$ foil. Accelerated protons also produced neutrons through the $^7$Li(p,n) reaction. Thus, the CR-39 fluences represent the sum of all neutrons generated in the experiment, not only through the $^7$Li(d,xn) reaction.

The neutron fluence extrapolated from simulations[8] of $4 \times 10^{10}$ n sr$^{-1}$ is much greater than the maximum of $8 \times 10^8$ n sr$^{-1}$ observed. As alluded to before, this is due to proton contaminants that were not included in the modeling, which reduce deuteron number and energy. Modeling shows that

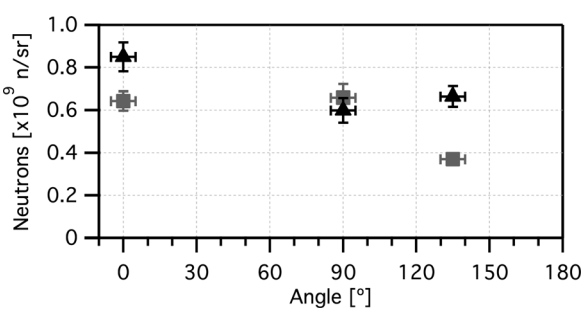


FIG. 5. Neutron fluences from experiment using CR-39 versus angle. The triangles (Shot 9) and squares (Shot 4) show data at the same nominal laser parameters (i.e., 360 J, 9 ps).

the neutron fluence increases with approximately the cube of deuteron energy and linearly with the number of deuterons.[15] The higher energy ions interact with the cross-section over a larger energy range and also their stopping power is lower at higher energy. Furthermore, the laser parameters in the experiment differ from those in the modeling. Thus, the discrepancy between neutron fluences is due to a number of factors described above, most likely dominated by the proton contaminant layer.

Additionally, our data shows only a small angular dependence of fluence. The expectation of a directional source comes from neutrons generated through the stripping process,[17] which creates a cone of forward directed neutrons. However, neutrons are only emitted in this manner if the incident deuteron exceeds the deuteron binding energy of 2.18 MeV, and the majority of the deuterons produced in this experiment do not fit these criteria. Again, removal of the contaminant layer would increase the deuteron energy and thus the directionality of the beam.

Several techniques have been used to reduce the proton contaminant layer including thermal heating[10] and Ar-ion sputtering.[18] A novel method to resolve this problem consists of applying artificial contaminants (e.g., $D_2O$) to replace the native ones.[19] Alternatively, large laser fluence ($>1$ J $\mu m^{-2}$) is expected to blow-off contaminants.[15]

In summary, we have shown acceleration of neutrons with energies up to 18 MeV using high-energy, short-pulse lasers, with spectrally integrated neutron fluence of up to $8 \times 10^8$ n $sr^{-1}$ in the forward direction. In future experiments, we will use calibrated detectors to obtain the fluence of neutrons above 10 MeV and improved nTOF detectors to measure the neutron spectrum. Work to increase the acceleration of deuterons by removing the contaminant layer will increase the fluence and directionality of high energy neutrons.

The staff of the Jupiter Laser Facility and Jack Topper of the External Dosimetry Lab at LLNL were instrumental in the execution of this work. Discussions with Professor Toshinori Yabuuchi and Professor Peter Norreys were especially beneficial. This work performed under the auspices of the U.S. Department of Energy by Lawrence Livermore National Laboratory under Contract DE-AC52-07NA27344, Naval Research Laboratory (NRL) under the 6.1 program, and the Office of Naval Research.

[1]L. J. Perkins, B. G. Logan, M. D. Rosen, M. D. Perry, T. Diaz de la Rubia, N. M. Ghoniem, T. Ditmire, P. T. Springer, and S. C. Wilks, Nucl. Fusion **40**, 1 (2000).
[2]A. Buffler, Radiat. Phys. Chem. **71**, 853 (2004).
[3]W. von Lensa, R. Nabbi, and M. Rossbach, *RED-IMPACT* (Forschungszentrum Jülich GmbH, Germany, 2008).
[4]K. L. Lancaster, S. Karsch, H. Habara, F. N. Beg, E. L. Clark, R. Freeman, M. H. Key, J. A. King, R. Kodama, K. Krushelnick, K. W. D. Ledingham, P. McKenna, C. D. Murphy, P. A. Norreys, R. Stephens, C. Stoeckl, Y. Toyama, M. S. Wei, and M. Zepf, Phys. Plasmas **11**, 3404 (2004).
[5]D. P. Higginson, J. M. McNaney, D. C. Swift, T. Bartal, D. S. Hey, R. Kodama, S. Le Pape, A. Mackinnon, D. Mariscal, H. Nakamura, N. Nakanii, K. A. Tanaka, and F. N. Beg, Phys. Plasmas **17**, 100701 (2010).
[6]M. Siebold, J. Hein, M. Hornung, S. Podleska, M. C. Kaluza, S. Bock, and R. Sauerbrey, Appl. Phys. B **90**, 431 (2008), and references therein.
[7]P. A. Norreys, A. P. Fews, F. N. Beg, A. R. Bell, A. E. Dangor, P. Lee, M. B. Nelson, H. Schmidt, M. Tatarakis, and M. D. Cable, Plasma Phys. Controlled Fusion **40**, 175 (1998).
[8]J. Davis, G. M. Petrov, Tz. Petrova, L. Willingale, A. Maksimchuk, and K. Krushelnick, Plasma Phys. Controlled Fusion **52**, 045015 (2010); J. Davis and G. M. Petrov, Phys. Plasmas **18**, 073109 (2011).
[9]J. Fuchs, P. Antici, E. D'Humières, E. Lefebvre, M. Borghesi, E. Brambrink, C. A. Cecchetti, M. Kaluza, V. Malka, M. Manclossi, S. Meyroneinc, P. Mora, J. Schreiber, T. Toncian, H. Pépin, and P. Audebert, Nat. Phys. **2**, 48 (2006).
[10]M. Hegelich, S. Karsch, G. Pretzler, D. Habs, K. Witte, W. Guenther, M. Allen, A. Blazevic, J. Fuchs, J. C. Gauthier, M. Geissel, P. Audebert, T. Cowan, and M. Roth, Phys. Rev. Lett. **89**, 85002 (2002).
[11]D. S. Hey, M. H. Key, A. J. Mackinnon, A. G. MacPhee, P. K. Patel, R. R. Freeman, L. D. Van Woerkom, and C. M. Castaneda, Rev. Sci. Instrum. **79**, 053501 (2008).
[12]D. C. Carroll, K. Jones, L. Robson, P. Mckenna, S. Bandyopadhyay, P. Brummitt, D. Neely, F. Lindau, O. Lundh, and C.-G. Wahlström, Rutherford Appleton Laboratory, Central Laser Facility Annual Report No. 2005/2006, (2006).
[13]J. F. Ziegler, J. P. Biersack, and M. Ziegler, *SRIM* (Lulu.com, 2008).
[14]A. Mančić, J. Fuchs, P. Antici, S. Gaillard, and P. Audebert, Rev. Sci. Instrum. **79**, 073301 (2008); I. Choi, C. Kim, J. Sung, I. Kim, T. Yu, S. Lee, Y. Jin, K. Pae, N. Hafz, and J. Lee, Meas. Sci. Technol. **20**, 115112 (2009).
[15]G. M. Petrov, L. Willingale, J. Davis, Tz. Petrova, A. Maksimchuk, and K. Krushelnick, Phys. Plasmas **17**, 103111 (2010).
[16]U. Fischer, M. Avrigeanu, P. Pereslavtsev, S. P. Simakov, and I. Schmuck, J. Nucl. Mater. **367**, 1531 (2007).
[17]R. Serber, Phys. Rev. **72**, 1008 (1947).
[18]M. Allen, P. K. Patel, A. Mackinnon, D. Price, S. Wilks, and E. Morse, Phys. Rev. Lett. **93**, 265004 (2004).
[19]B. Hou, J. A. Nees, Z. He, G. Petrov, J. Davis, J. H. Easter, A. G. Thomas, and K. M. Krushelnick, Phys. Plasmas **18**, 040702 (2011).